Neurons derived from reprogrammed fibroblasts functionally integrate into the fetal brain and improve symptoms of rats with Parkinson's disease

Marius Wernig*, Jian-Ping Zhao†, Jan Pruszak‡, Eva Hedlund‡, Dongdong Fu*, Frank Soldner*, Vania Broccoli§, Martha Constantine-Paton†, Ole Isacson‡, and Rudolf Jaenisch*¶‖

*The Whitehead Institute for Biomedical Research, Cambridge, MA 02142; †The McGovern Institute for Brain Research and ¶Department of Biology, Massachusetts Institute of Technology, Cambridge, MA 02139; ‡Udall Parkinson's Disease Research Center of Excellence and Neuroregeneration Laboratories, McLean Hospital/Harvard University, Belmont, MA 02478; and §San Raffaele Scientific Institute, 20132 Milan, Italy

Contributed by Rudolf Jaenisch, February 21, 2008 (sent for review January 21, 2008)

The long-term goal of nuclear transfer or alternative reprogramming approaches is to create patient-specific donor cells for transplantation therapy, avoiding immunorejection, a major complication in current transplantation medicine. It was recently shown that the four transcription factors Oct4, Sox2, Klf4, and c-Myc induce pluripotency in mouse fibroblasts. However, the therapeutic potential of induced pluripotent stem (iPS) cells for neural cell replacement strategies remained unexplored. Here, we show that iPS cells can be efficiently differentiated into neural precursor cells, giving rise to neuronal and glial cell types in culture. Upon transplantation into the fetal mouse brain, the cells migrate into various brain regions and differentiate into glia and neurons, including glutamatergic, GABAergic, and catecholaminergic subtypes. Electrophysiological recordings and morphological analysis demonstrated that the grafted neurons had mature neuronal activity and were functionally integrated in the host brain. Furthermore, iPS cells were induced to differentiate into dopamine neurons of midbrain character and were able to improve behavior in a rat model of Parkinson's disease upon transplantation into the adult brain. We minimized the risk of tumor formation from the grafted cells by separating contaminating pluripotent cells and committed neural cells using fluorescence-activated cell sorting. Our results demonstrate the therapeutic potential of directly reprogrammed fibroblasts for neuronal cell replacement in the animal model.

embryonic stem cells | epigenetic | induced pluripotent stem cells | reprogramming | cell transplantation

Embryonic stem (ES) cells can be expanded to virtually unlimited numbers and have the potential to generate all cell types in culture. Therefore, ES cells are an attractive new donor source for transplantation and hold promise to revolutionize regenerative medicine (1). The ES cell based therapy is complicated, however, by immune rejection due to immunological incompatibility between patient and donor ES cells. The successful generation of cloned stem cells and animals by somatic cell nuclear transfer (SCNT) created the possibility to generate genetically identical "customized" SCNT-ES cells by using donor cells from a patient (2, 3). This strategy would eliminate the requirement for immune suppression. Despite successful application of SCNT-ES cells in animal disease models, both technical and logistic impediments as well as ethical considerations of the nuclear transfer procedure complicate the practical realization of "therapeutic SCNT" in human (4–7).

Recently, *in vitro* reprogramming of mouse fibroblasts into pluripotent stem cells [induced pluripotent stem (iPS) cells] was achieved through retroviral transduction of the four transcription factors Oct4, Sox2, c-Myc, and Klf4 and selection for reactivation of the ES cell marker gene Fbx15 (8). When selected for endogenous reexpression of the key pluripotency genes Oct4 or Nanog, reprogrammed fibroblasts were indistinguishable from blastocyst-derived embryonic stem cells both in terms of their epigenetic state and their developmental potential (9–12).

The ultimate goal of somatic reprogramming is to generate functional cell types relevant for therapy such as neurons, cardiomyocytes, insulin-producing cells, or hematopoietic cells *in vitro*. In a recent proof of principle study, we could demonstrate a therapeutic benefit of iPS cell-derived hematopoietic cells in a humanized mouse model of sickle cell anemia (13). Cell replacement therapy seems particularly suitable for Parkinson's disease, a common neurodegenerative disease caused by loss of midbrain dopamine neurons (14–16). Transplantation of fetal midbrain cells has been shown to restore dopamine function in animal models and in human patients (17–22). More recently, also dopamine neurons derived from embryonic stem cells have been shown to function when grafted into parkinsonian rats (23–25). To evaluate their therapeutic potential, we therefore tested whether functional neurons can be generated from reprogrammed fibroblasts *in vitro*. Our data show that iPS cell-derived neurons synaptically integrate after transplantation into the fetal mouse brain and function after transplantation into the adult brain in a rat model of Parkinson's disease.

Results

Reprogrammed Fibroblasts Robustly Differentiate into Neural Lineages *in Vitro*. To test the neural differentiation potential of reprogrammed fibroblasts *in vitro*, we chose the Nanog-selected iPS cell lines N8, N10, and N14, the Oct4-selected iPS cell lines O9 and O18 (11), as well as the non-drug-selected iPS cell line OG-14 (12), and applied a multistage differentiation protocol that had been previously developed in ES cells (26). After initial expansion on irradiated MEF feeder cells (Fig. 1*a*), the iPS cells were passaged onto gelatin-coated dishes to purify from feeder cells and were transferred to nonadherent culture dishes where they readily formed spheroid embryoid bodies. Upon plating and culture in serum-free media the cells formed clusters of neuroepithelial-like cells that could be isolated and propagated in FGF2-containing media. These cells showed a typical neural precursor cell morphology (Fig. 1*b*) and homogeneously expressed the neural stem cell marker proteins nestin, Sox2, and Brn2 [supporting information (SI) Fig. S1]. Seven days after withdrawal of FGF2, the cells had robustly differentiated into

Author contributions: J.-P.Z. and J.P. contributed equally to this work; M.W., O.I., and R.J. designed research; M.W., J.-P.Z., J.P., E.H., D.F., F.S., and V.B. performed research; M.W., J.-P.Z., J.P., E.H., D.F., M.C.-P., and O.I. analyzed data; and M.W., M.C.-P., O.I., and R.J. wrote the paper.

The authors declare no conflict of interest.

‖To whom correspondence should be addressed at: The Whitehead Institute for Biomedical Research, 9 Cambridge Center, Cambridge, MA 02142. E-mail: jaenisch@wi.mit.edu.

This article contains supporting information online at www.pnas.org/cgi/content/full/0801677105/DCSupplemental.

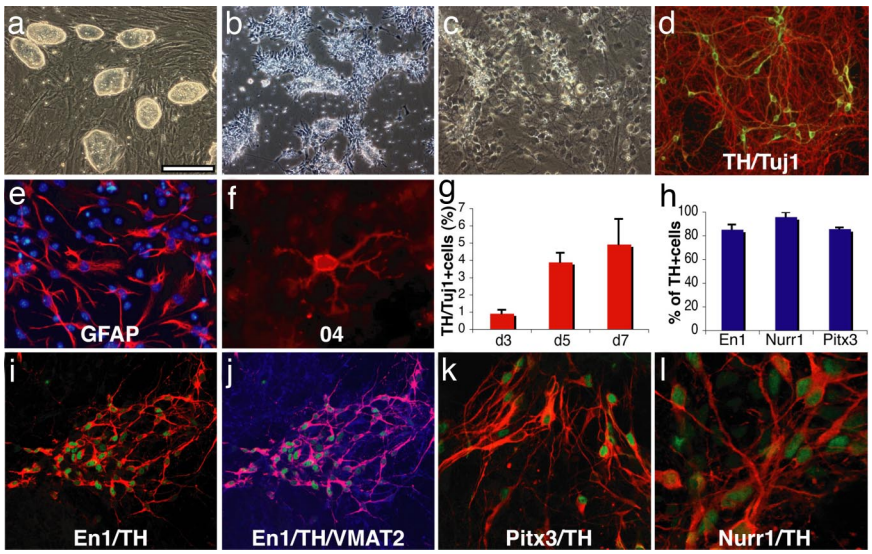

Fig. 1. *In vitro* differentiation of induced pluripotent stem cells. (*a*) The undifferentiated Oct4-selected iPS cell line O9. (*b*) FGF2-responsive neural precursor cells. (*c*) Differentiated neural morphologies 7 days after growth factor withdrawal. (*d*) A fraction of β-III-tubulin positive neurons (red) are double labeled with antibodies against TH (green, yellow in merged image), 7 days after growth factor withdrawal. (*e* and *f*) At this stage, also, many GFAP-positive astrocytes (red) (*e*) and rare 04-positive oligodendrocytes (*f*) are found. (*g*) The fraction of TH-positive cells over β-III-tubulin positive cells increases along neuronal maturation (mean and standard deviation, three independent experiments). (*h*) The vast majority of TH-immunoreactive cells coexpress En1, Pitx3, and Nurr1 (mean, standard deviation). (*i*) Coexpression of En1 (green) and TH (red). (*j*) VMAT2 and TH [purple in the merged image indicates colocalization of TH (red) and VMAT2 (blue)]. (*k* and *l*) Most TH-positive cells (red) are also positive for Pitx3 (green) (*k*), and Nurr1 (green) (*l*) after 7 days of neuronal differentiation. [Scale bar in *a*: 200 μm (*a* and *b*), 100 μm (*c*, *d*, *i*, and *j*), 50 μm (*e* and *k*), and 20 μm (*f* and *l*).]

β-III-tubulin-positive neurons, glial fibrillary acidic protein (GFAP)-positive astrocytes and 04-positive oligodendrocytes (Fig. 1 *c–f*).

We then tested whether iPS cells have the capacity to give rise to clinically relevant neuronal subtypes such as dopamine neurons of midbrain character. Following protocols developed for mouse ES cells, we treated FGF2 responsive, iPS cell-derived neural precursor cells with the regional patterning factors sonic hedgehog and FGF8 (23, 27). After withdrawal of the growth and patterning factors most cells differentiated into β-III-tubulin-positive cells with neuronal morphology, a fraction of which could also be labeled with antibodies against tyrosine hydroxylase (TH) (Fig. 1*d*). Quantification of three independent experiments revealed that the number of TH-positive neurons increased over time in culture (Fig. 1*g*). These cells also expressed the vesicular monoamine transporter 2 (VMAT2) that is responsible for catecholamine transport into synaptic vesicles (Fig. 1*j*). To assess their regional specification we double-labeled TH-positive neurons with antibodies against En1, Pitx3, and Nurr1, all markers typically expressed in dopamine neurons of the midbrain. Importantly, the vast majority of TH-positive cells stained for these three midbrain markers suggesting their proper regional specification *in vitro* (Fig. 1 *i*, *k*, and *l*).

iPS Cell-Derived Neural Precursor Cells Extensively Migrate and Differentiate into Neurons and Glia After Transplantation into the Developing Brain. We derived neural precursor cells from iPS cells that had been infected with a GFP-expressing lentivirus (28). To explore their migratory capacity, 100,000–300,000 FGF2 responsive neural precursor cells derived from the GFP-positive iPS cell subclones N8.2, N14.2 and O9.2 were transplanted *in utero* into the lateral brain ventricles of embryonic day (E) 13.5–E14.5 mouse embryos. Transplanted mice were spontaneously delivered and analyzed one to nine weeks after surgery. As shown in Fig. 2*a* transplanted cells formed intraventricular clusters and some had migrated extensively into the surrounding brain tissue. GFP-positive cells were found in many different brain regions. The highest densities of transplanted cells were found in septum, striatum, hypothalamus and midbrain. Smaller numbers were detected in olfactory bulb, cortex and thalamus and no cells were found in cerebellum and brainstem (Fig. 2 *a–c* and *g* and Table 1). Incorporated cells displayed various complex neuronal and glial morphologies (Fig. 2 *c–f*) expressing the neuronal marker proteins NeuN and β-III-tubulin or the glial marker GFAP (Fig. 3 *a–c*). The engrafted neurons gave rise to various neuronal subtypes including glutamate transporter EAAC1-positive glutamatergic neurons, Glutamic acid decarboxylase 67 (GAD67)-positive GABAergic neurons and TH-positive catecholaminergic neurons (Fig. 3 *d–f*).

Transplanted iPS Cell-Derived Neurons Are Functionally Integrated in the Host Brain. First, we sought morphological evidence of neuronal maturity and synaptic integration of transplanted iPS cell-derived neurons. Immunofluorescent labeling for GFP provided a crisp outline of the incorporated cells, clearly delineating their shapes and fine neuronal processes (Fig. 2 *e* and *f* and Fig. 4 *a* and *b*). Confocal analysis demonstrated the presence of small synaptic spines on the surface of dendritic processes and numerous synaptophysin-positive, GFP-negative patches were found in close apposition to the somatic and dendritic membranes of transplanted cells, suggesting that host-derived presynaptic terminals contacted iPS cell-derived neurons (Fig. 4*c*).

Electrophysiological recordings from brain slices prepared from transplanted animals were used to examine functional neuronal properties in the engrafted cells. GFP-positive cells with long dendrite-like processes were identified as neurons by focusing through the depth of the tissue (Fig. 4*d*). All cells recorded from two animals were in the central region of the inferior colliculus. To properly place the electrode, the microscope was switched to infrared differential interference contrast in the plane of the cell body (Fig. 4*e*). Cell-attached voltage-clamp recordings were made in three GFP-positive cells. All three cells showed spontaneous action potential currents (Fig. 4*e*

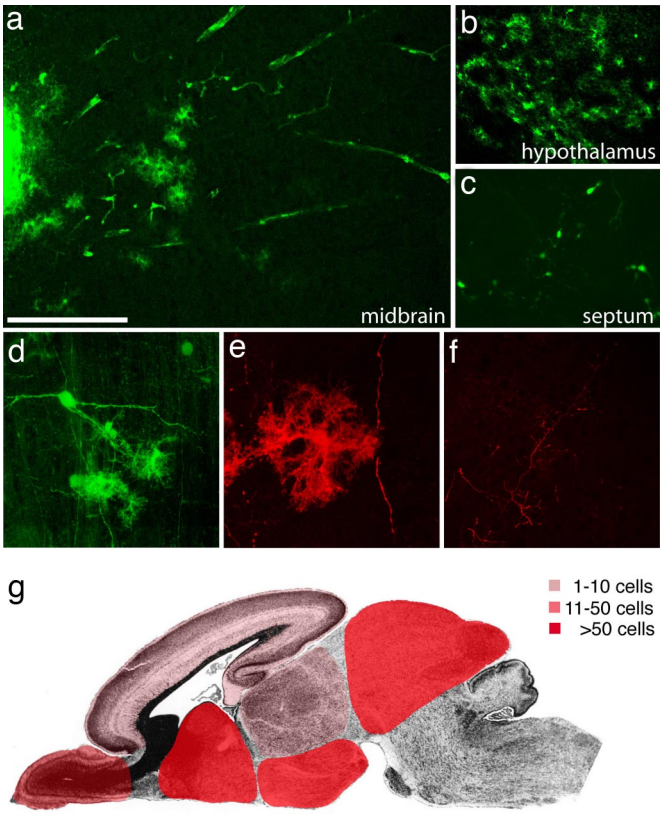

Fig. 2. Extensive migration and differentiation of iPS cell-derived neural precursor cells in the embryonic brain. (*a*) Transplanted cells form an intraventricular cluster (left part of the image) and migrate extensively into the tectum 4 weeks after transplantation into the lateral brain ventricles of E13.5 mouse embryos. (*b*) A high density of integrated astrocyte-like cells in the hypothalamus. (*c*) Complex neuronal morphologies of GFP-positive cells in the septum. (*d*) Confocal reconstruction of grafted GFP-fluorescent cells in the tectum with neuronal and glial morphologies. (*e*) GFP immunofluorescence and confocal reconstruction identifies an astrocytic cell and a long neuronal process. (*f*) Similarly, GFP-immunoreactive, fine neuronal processes are crisply delineated. (*g*) Schematic representation of the main integration sites of iPS cell-derived neurons and glia. Color codes represent different ranges of cell numbers. Shown are the highest incorporation density across all analyzed brains. See Table 1 for more details. [Scale bar in *a*: 200 μm (*a–c*), 100 μm (*d* and *f*), and 50μ (*e*).]

Inset). Synaptic inputs were examined in an additional six cells held in voltage clamp at −70 mV. All cells showed spontaneous postsynaptic currents ranging in amplitude and kinetics and therefore indicative of inputs from different ionotropic transmitter receptor types. At −70 mV, with our recording solutions, inward currents will reflect both inhibitory and excitatory synaptic activity (Fig. 4*f*). To test the active membrane characteristics of the labeled cells recordings were switched to current clamp mode. Resting membrane potentials of these cells ranged from −53 to −63 mV (−60 ± 2.4 mV). For current injection experiments the resting membrane potential was shifted to the more polarized potential of −68 mV. Starting from this potential, depolarizing current injections induced action potentials ranging in amplitude from 70 to 82 mV (78.8 ± 2.9 mV). Thresholds for action potential initiation were in the range of −40 mV (Fig. 4*g*).

Functional Recovery of Parkinsonian Rats After Transplantation of iPS Cell-Derived Midbrain Dopamine Neurons. One of the prime candidate diseases for cell replacement therapy is Parkinson's disease because of the rather localized degeneration of a specific cell type (16, 29–32). We therefore asked whether injected iPS cells were able to restore function after loss of endogenous midbrain dopaminergic neurons in the adult brain. In rats, administration of 6-hydroxy dopamine (6-OH-DA) into the striatum specifically kills dopamine neurons, providing a useful model of Parkinson's disease.

Table 1. Incorporation of iPS cell-derived neurons and glia after *in utero* transplantation

Animal	Age	OB	CTX	SPT	TH	HT	MB	CB/BS
329.1	P0	++	+	−	+	−	++	−
329.2	P0	−	+	−	−	−	−	−
1855.1	P0	−	−	−	+	+	−	−
1856.3	P0	−	−	+	−	+	−	−
1870.1	P27	−	++	+	−	++	−	−
1865.1	P29	−	++	+++	−	+++	+++	−
1865.3	P29	−	++	++	+	+++	−	−
1857.2	P56	−	+	++	++	+	−	−
1857.3	P56	−	+	++	−	−	−	−
1857.4	P56	ND	ND	ND	ND	ND	+++	−

Cells were transplanted at E13.5, and brains were analyzed at the indicated postnatal day (P). The brains were serially sectioned, and cells incorporated into the brain parenchyma (located at least 50 μm from clusters or the ventricular wall) were counted. Indicated are the maximum number of cells on a 50-μm section from at least three sections per brain region. −, no cells; +, 1–10 cells; ++, 11–50 cells; +++, >50 cells. OB, olfactory bulb; CTX, cortex; SPT, septum; TH, thalamus; HT, hypothalamus; MB, midbrain; CB, cerebellum; BS, brain stem; ND, not done.

Reprogrammed fibroblasts (iPS cell clone O9) were differentiated into dopamine neurons as described above and animals lesioned with 6-OH-DA either received a sham operation or a striatal graft of 1–3 × 10^5 differentiated cells 5 days after the cells were withdrawn from the growth and patterning factors (stage 5, day 5). Four weeks after surgery, animals were used for morphological analysis with TH immunostaining. Sham-grafted animals showed no TH-positive elements in the ipsilateral substantia nigra or the dorsal striatum. In contrast, in the striatum of rats grafted with differentiated iPS cells, a large number of TH-positive cells were found (Fig. 5*a*). These cells showed complex morphologies (Fig. 5*b*) and were also positive for En1, VMAT2, and dopamine transporter (DAT) (Fig. 5 *e–g*). The somata of TH-positive cells remained in close vicinity of the graft but TH-immunoreactive fibers were found to extend into the parenchyma of the host striatum (Fig. 5*b*; dashed line delineates the border zone of the graft).

We next examined the behavior of sham-operated rats and rats grafted with dopamine neurons derived from iPS cells. Amphetamine stimulation to animals lesioned unilaterally with 6-OH-DA induces a movement bias ipsilateral to the injection site. Whereas the control group showed a stable rotational bias over time, four of five transplanted animals showed a marked recovery of the rotation behavior 4 weeks after transplantation (Fig. 5*b* and Fig. S2). All four responding animals contained large numbers of TH-positive neurons in contrast to the one nonresponding animal. Cell counts in serial sections from one representative responding animal revealed that this graft contained an estimated total number of ≈29,000 TH-positive neurons whereas only ≈1,500 TH-positive cells were estimated to have been present in the nonresponding animal. In the latter animal, despite a relatively high number of DA neurons in the large graft, they were typically located in the center of the graft, and so very few DA fibers extended to the host striatum. Consequently, only marginal innervation (≤10%) of the dopamine-depleted striatum was achieved, which might be the reason for lack of functional recovery at this time point.

Immunohistochemical examination revealed graft areas containing Ki67-positive cells in all five animals that showed func-

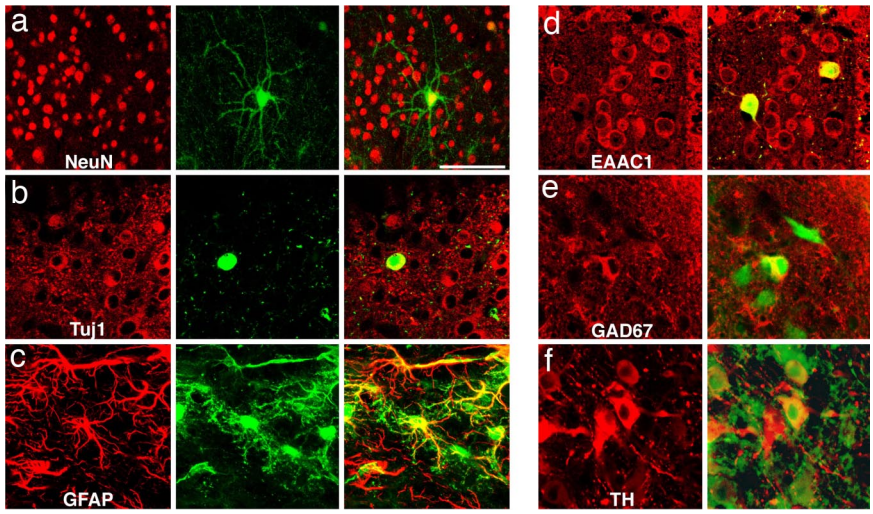

Fig. 3. Transplanted cells express neuronal and glial markers. (*a*) Confocal reconstruction of a GFP-positive cell in the midbrain (green) expressing NeuN (red) 4 weeks after intrauterine transplantation. (*b*) Another transplanted neuron (green) expresses cytoplasmatic β-III-tubulin (red) as shown in this confocal section. (*c*) Other cells can be colabeled with GFAP antibodies (red). (*d*) Both host neurons (red only) and transplanted cells (yellow) express the glutamate transporter EAAC1. (*e*) Soma of grafted cells (green) can be labeled with antibodies against GAD67 (red). (*f*) TH-immunoreactivity (red) can be found in both host and grafted neurons (green). [Scale bar in *a*: 100 μm (*a–c*) and 50 μm (*d–f*).]

tional recovery and in two of five animals from another set of transplantations indicating the continuous proliferation of transplanted cells. Upon close morphological examination, we identified histological structures of nonneural tissue suggesting the presence of teratoma formations (Fig. S3 *a–f*). The contamination of undifferentiated ES cells and subsequent teratoma formation after transplantation still seems to be a major complication of ES cell-based therapies in animal transplantation models (24, 33–35). This complication seems the most likely reason for teratoma formation also in our experiments as the viral transcripts were not reactivated in those tumors (Fig. S3*j*). Indeed, when we reanalyzed our cultures at the stages used for transplantation (≈3 weeks of differentiation), we did find rare and small clusters of undifferentiated Nanog-positive cells although the vast majority of these cultures contained postmitotic neurons (Fig. S3 *g–i*). We therefore reasoned that elimination of undifferentiated cells from the cultures should lead to a reduction in the risk of teratoma formation after transplantation. To this end, FACS was used to deplete the cell suspension from SSEA1-positive cell fraction before transplantation (Fig. S4*a*). Cultures established from sorted cells showed decreased presence of undifferentiated cell types, and a network of differentiated neurons as soon as one day after plating (Fig. S4*b*). Four animals grafted with iPS cell-derived neuronal cell preparations depleted of SSEA1-positive cells recovered at degrees similar to animals receiving nonpurified cell suspensions (Fig. 5*d* and Fig. S2*b*). Histologically, the grafts were consistently smaller and no tumor formation was observed up to 8 weeks after transplantation (Fig. S4*c*).

Discussion

In the current study, we have shown that mouse fibroblasts reprogrammed by retroviral transduction of the four transcription factors Oct4, Sox2, Klf4, and c-Myc can differentiate into functional neurons *in vitro*. When injected into embryonic cerebral ventricles iPS cell-derived neural precursor cells migrated into various brain regions and differentiated into glia and neurons. Whole cell recordings in slices demonstrated that iPS cell-derived neurons are synaptically integrated into the host brain and show active action potential generating membrane properties. The widespread integration pattern suggests a wide spectrum of neuronal differentiation potential (36, 37), but nonorthotopic expression of regional markers has been detected in ES cell-derived neurons, emphasizing the importance of neuronal subtype prespecification before transplantation (38). In the directed differentiation of the iPS cells, the presence of several midbrain-type neurons was further explored for therapeutic potential by transplantation to an adult animal model of dopamine neuron loss, as an analogy of behavioral deficits in Parkinson's disease. The successful implantation and functional recovery in such animals is evidence for the therapeutic value of directly reprogrammed fibroblasts for cell replacement strategies in the adult brain.

The efficiency of our cell transplantation therapy was striking: eight of the nine transplanted and behaviorally tested animals contained high numbers of TH-positive cells with local innervation of the host brain and showed improvement in the behavior test. One animal showed an even higher dopamine activity of the graft compared with the endogenous activity in the contralateral side (Fig. S2). Importantly, however, serious safety issues with this therapeutic approach need to be addressed in the future. First, alternative delivery methods of the pluripotency-inducing factors will have to developed because retroviral vectors are randomly integrating into the genome and the potential retrovirus reactivation in transplanted cells could lead to cancerous transformation of transplanted neurons. Indeed, 16 of the 36 iPS cell chimeras generated in our laboratory have died within the first 8 months of age, many of which had developed a tumor of variable location and histological appearance (M.W. and R.J., unpublished results). Similarly, Yamanaka's group reported the retroviral reactivation of c-Myc and neck tumor formation in a fraction of their F1 germ-line iPS cell mice (10). A safer alternative for the future would be the development of DNA-free protocols to induce pluripotency such as through action of small molecules or engineered membrane permeable transcription factor proteins. In the current study, we noticed also the risk of teratoma formations due to the contamination of a small proportion of undifferentiated cells. This contamination represents another frequent complication of ES cell transplantations (24, 33–35, 39). The retroviruses incorporated into the iPS cell genome were not reactivated in these tumors. Using stringent cell sorting for SSEA1-negative cells, we succeeded in reducing

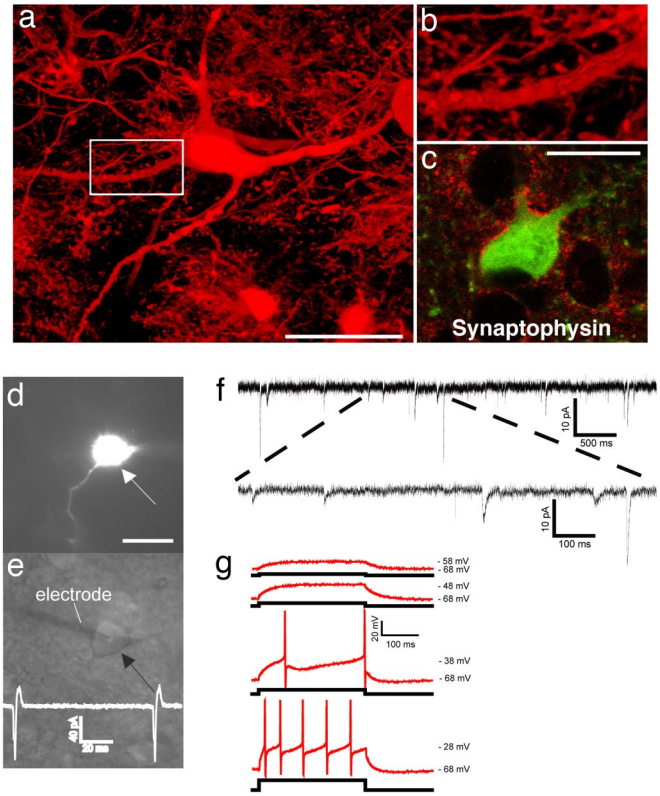

Fig. 4. Synaptic integration of functional iPS cell-derived neurons into the host brain. (*a*) GFP-immunofluorescence allows the high resolution characterization of dendritic morphologies of transplanted neurons. (*b*) Higher magnification of the indicated part in *a* suggests the presence of synaptic spines along this dendrite. (*c*) Integrated GFP-positive neurons are adjacent to many synaptophysin-positive patches (red), indicating synaptic contacts from host axon terminals. (*d*) A GFP-expressing neuron (arrow) in the dorsal midbrain was detected in acute brain slices of a P20 mouse brain after *in utero* transplantation. (*e*) GFP-positive neurons were identified by infrared differential interference contrast (arrow) and approached by a recording electrode (left). The trace indicates spontaneous generation of action potentials. (*f*) Voltage-clamp recording at −70 mV in extracellular solution containing 3 mM Mg^{2+}. Traces show spontaneous slow and fast currents that indicate that this transplanted neuron receives synaptic contacts from host cells. All six recorded GFP-positive neurons from two mice (age P20 and P22) exhibited similar spontaneous currents. (*g*) Current-clamp recordings during current injection. Shown are superimposed membrane potential changes (*Upper* traces, red), which demonstrates the capability of the grafted neurons to fire action potentials in response to a series of current injection (*Lower* traces, black) from a holding potential of −68 mV. All six analyzed GFP-neurons showed these active membrane characteristic. (Scale bars: 20 μm.)

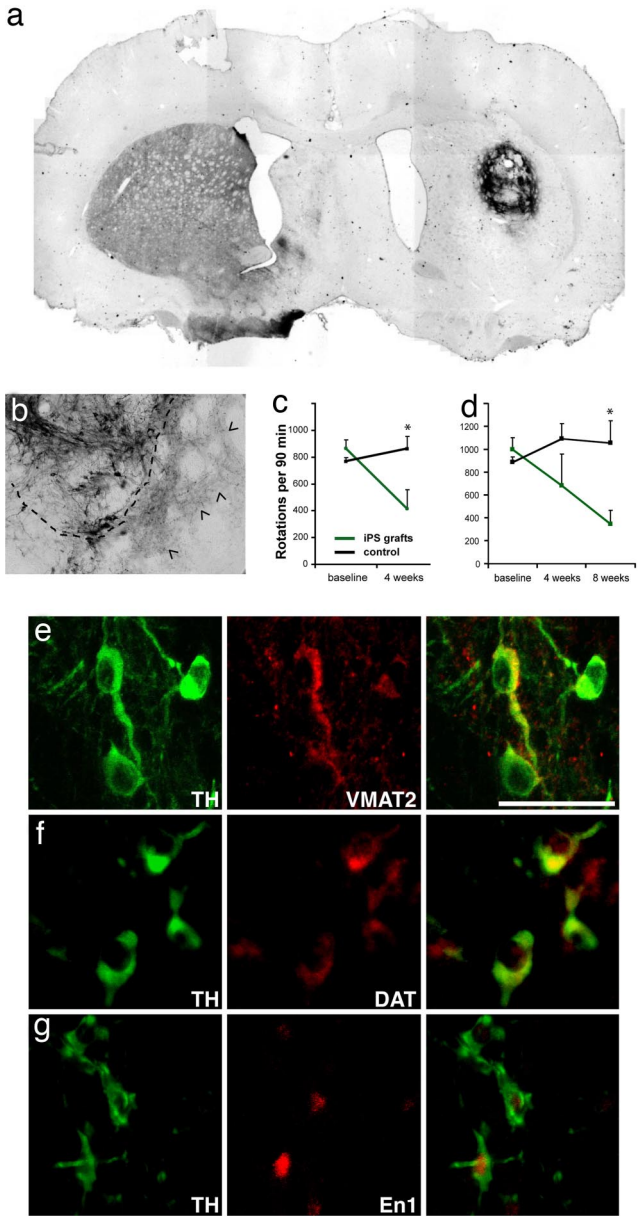

Fig. 5. iPS cell-derived neurons integrate into the striatum of hemiparkinsonian rats and improve behavioral deficits. (*a*) Overview of an iPS cell graft 4 weeks after transplantation stained with antibodies against TH (dark brown). (*b*) Higher magnification of another graft showing TH-positive soma and the dense innervation of the surrounding host striatum by donor-derived neurites (arrowheads). The dashed line indicates the edges of the graft. (*c*) Amphetamine-induced rotations are significantly reduced in animals grafted with unsorted iPS cell populations (green, $n = 5$) compared with the sham control animals (black, $n = 10$) ($P = 0.0185$, unpaired Student's t test). Shown are the number of rotations in 90 min after amphetamine injection as means and standard deviations. (*d*) Amphetamine-induced rotations in animals transplanted with iPS cell cultures after elimination of SSEA1-positive cells by FACS. Grafted animals (green, $n = 4$) show significant recovery compared with control animals (black, $n = 10$) ($P = 0.006$). (*e–g*) The grafted TH-positive cells (green) can be colabeled (red) with antibodies against VMAT2 (*e*), DAT (*f*), and En1 (*g*). (Scale bar: 50 μm.)

the number of contaminating undifferentiated iPS cells from the neural cell cultures. The elimination of undifferentiated cells led to a substantially reduced risk of teratoma formation after transplantation: we failed to detect teratomas in any of the transplanted rats at 8 weeks after transplantation whereas the animals exhibited a similar recovery rate in the behavior test compared with the animals receiving unsorted cell populations.

One notable potential risk of therapeutic reprogramming is that thus far unknown genetic factors causing the patient's disease could also potentially lead to degeneration of the reprogrammed and transplanted cells. But in light of the late onset of most neurodegenerative diseases in the range of multiple decades, this possible complication might not have a critical impact during the lifetime of a treated patient.

Generation of chimeric brains composed of WT and iPS cell-derived neurons by intrauterine transplantation provides the interesting prospect to study disease neurons on the cellular level *in vivo*. For instance, skin cells from patients suffering from complex neurodegenerative disorders could be reprogrammed, differentiated into neurons and glia and introduced into the developing nervous system. The properties of these cells could then be assayed

in vivo in a WT recipient brain as suggested for mouse and human ES cells previously (40, 41). The data presented here indicate that a large range of neuronal and glial phenotypes could be studied with this approach. Also, the efficient and highly localized cell transfer will allow the targeted introduction of patient-derived neurons into defined brain regions.

In summary, our findings demonstrate that direct reprogramming is functionally equivalent to "therapeutic cloning" by nuclear transfer but many important complications need to be eliminated before this technique can be safely applied in human.

Methods

***In Vitro* Differentiation, Transplantation, Behavioral Analysis, and Immunofluorescence.** iPS cells were differentiated as described for ES cells (26, 27). The surgical procedures have been described in detail before in refs. 36, 39, and 40. 6-OH-DA-lesioned animals were placed into automated rotometer bowls, and left and right full-body turns were monitored for 90 min after a single dose of amphetamine (4 mg/kg) by a computerized activity monitor system. All animal studies were performed following National Institutes of Health guidelines and were approved by the Institutional Animal Care and Use Committee at McLean Hospital and Harvard Medical School. Immunofluorescence analysis was performed following standard protocols. Detailed information is listed in *SI Methods*.

Electrophysiology. Parasagittal brain slices from grafted P20 and P22 mice were screened for GFP-positive neuron-like cells by using a fluorescence camera (CoolSNAP EZ; Photometrics, Ottobrunn, Germany), were subsequently visualized by using infrared differential interference contrast optics and recorded following standard procedures. Detailed recording parameters are listed in *SI Methods*.

ACKNOWLEDGMENTS. We thank Casper Reske-Nielsen, Wesley Ludwig, and Jessica Dausman for outstanding technical assistance, as well as Jacob Hanna, Menno Creighton, and Chris Lengner for helpful comments on the manuscript. M.W. was supported by the Allison Foundation. R.J. was supported by National Institutes of Health (NIH) Grants R01-CA087869, R37-CA084198, and R01-HD0445022. O.I. was supported by NIH Grant P50NS39793, The Michael Stern Foundation, The Orchard Foundation, The Consolidated Anti-Aging Foundation, and The Harold and Ronna Cooper Family. V.B. was supported by Telethon Grant GGP07181.

1. Lerou PH, Daley GQ (2005) Therapeutic potential of embryonic stem cells. *Blood Rev* 19:321–331.
2. Hochedlinger K, Jaenisch R (2003) Nuclear transplantation, embryonic stem cells, and the potential for cell therapy. *N Engl J Med* 349:275–286.
3. Jaenisch R (2004) Human cloning: The science and ethics of nuclear transplantation. *N Engl J Med* 351:2787–2791.
4. Weissman IL (2006) Medicine: Politic stem cells. *Nature* 439:145–147.
5. Rideout WM, III, Hochedlinger K, Kyba M, Daley GQ, Jaenisch R (2002) Correction of a genetic defect by nuclear transplantation and combined cell and gene therapy. *Cell* 109:17–27.
6. Wakayama T, *et al*. (2001)Differentiation of embryonic stem cell lines generated from adult somatic cells by nuclear transfer. *Science* 292:740–743.
7. Barberi T, *et al*. (2003) Neural subtype specification of fertilization and nuclear transfer embryonic stem cells and application in parkinsonian mice. *Nat Biotechnol* 21:1200–1207.
8. Takahashi K, Yamanaka S (2006) Induction of pluripotent stem cells from mouse embryonic and adult fibroblast cultures by defined factors. *Cell* 126:663–676.
9. Maherali N, *et al*. (2007) Global epigenetic remodeling in directly reprogrammed fibroblasts Cell. *Stem Cell* 1:55–70.
10. Okita K, Ichisaka T, Yamanaka S (2007) Generation of germline-competent induced pluripotent stem cells. *Nature* 448:313–317.
11. Wernig M, *et al*. (2007) *In vitro* reprogramming of fibroblasts into a pluripotent ES-cell-like state. *Nature* 448:318–324.
12. Meissner A, Wernig M, Jaenisch R (2007) Direct reprogramming of genetically unmodified fibroblasts into pluripotent stem cells. *Nat Biotechnol* 25:1177–1181.
13. Hanna J, *et al*. (2007) Treatment of sickle cell anemia mouse model with iPS cells generated from autologous skin. *Science* 318:1920–1923.
14. Lindvall O, Kokaia Z (2006) Stem cells for the treatment of neurological disorders. *Nature* 441:1094–1096.
15. Winkler C, Kirik D, Bjorklund A (2005) Cell transplantation in Parkinson's disease: How can we make it work? *Trends Neurosci* 28:86–92.
16. Isacson O (2003) The production and use of cells as therapeutic agents in neurodegenerative diseases. *Lancet Neurol* 2:417–424.
17. Parish CL, *et al*. (2008) Wnt5a-treated midbrain neural stem cells improve dopamine cell replacement therapy in parkinsonian mice. *J Clin Invest* 118:149–160.
18. Bjorklund LM, Isacson O (2002) Regulation of dopamine cell type and transmitter function in fetal and stem cell transplantation for Parkinson's disease. *Prog Brain Res* 138:411–420.
19. Freed CR, *et al*. (2001) Transplantation of embryonic dopamine neurons for severe Parkinson's disease. *N Engl J Med* 344:710–719.
20. Piccini P, *et al*. (1999) Dopamine release from nigral transplants visualized *in vivo* in a Parkinson's patient. *Nat Neurosci* 2:1137–1140.
21. Lee CS, Cenci MA, Schulzer M, Bjorklund A (2000) Embryonic ventral mesencephalic grafts improve levodopa-induced dyskinesia in a rat model of Parkinson's disease. *Brain* 123:1365–1379.
22. Mendez I, *et al*. (2005) Cell type analysis of functional fetal dopamine cell suspension transplants in the striatum and substantia nigra of patients with Parkinson's disease. *Brain* 128:1498–1510.
23. Kim JH, *et al*. (2002) Dopamine neurons derived from embryonic stem cells function in an animal model of Parkinson's disease. *Nature* 418:50–56.
24. Roy NS, *et al*. (2006) Functional engraftment of human ES cell-derived dopaminergic neurons enriched by coculture with telomerase-immortalized midbrain astrocytes. *Nat Med* 12:1259–1268.
25. Yang D, Zhang ZJ, Oldenburg M, Ayala M, Zhang SC (2008) Human embryonic stem cell-derived dopaminergic neurons reverse functional deficit in parkinsonian rats. *Stem Cells* 26:55–63.
26. Okabe S, Forsberg-Nilsson K, Spiro AC, Segal M, McKay RD (1996) Development of neuronal precursor cells and functional postmitotic neurons from embryonic stem cells *in vitro*. *Mech Dev* 59:89–102.
27. Lee SH, Lumelsky N, Studer L, Auerbach JM, McKay RD (2000) Efficient generation of midbrain and hindbrain neurons from mouse embryonic stem cells. *Nat Biotechnol* 18:675–679.
28. Lois C, Hong EJ, Pease S, Brown EJ, Baltimore D (2002) Germline transmission and tissue-specific expression of transgenes delivered by lentiviral vectors. *Science* 295:868–872.
29. Marsden CD (1994) Problems with long-term levodopa therapy for Parkinson's disease. *Clin Neuropharmacol* 17(Suppl 2):S32–S44.
30. Fearnley JM, Lees AJ (1991) Ageing and Parkinson's disease: Substantia nigra regional selectivity. *Brain* 114:2283–2301.
31. Pakkenberg B, Møller A, Gundersen HJ, Mouritzen Dam A, Pakkenberg H (1991) The absolute number of nerve cells in substantia nigra in normal subjects and in patients with Parkinson's disease estimated with an unbiased stereological method. *J Neurol Neurosurg Psychiatry* 54:30–33.
32. German DC, Manaye K, Smith WK, Woodward DJ, Saper CB (1989) Midbrain dopaminergic cell loss in Parkinson's disease: Computer visualization. *Ann Neurol* 26:507–514.
33. Erdo F, *et al*. (2003) Host-dependent tumorigenesis of embryonic stem cell transplantation in experimental stroke. *J Cereb Blood Flow Metab* 23:780–785.
34. Hedlund E, *et al*. (2007) Selection of embryonic stem cell-derived enhanced green fluorescent protein-positive dopamine neurons using the tyrosine hydroxylase promoter is confounded by reporter gene expression in immature cell populations. *Stem Cells* 25:1126–1135.
35. Pruszak J, Sonntag KC, Aung MH, Sanchez-Pernaute R, Isacson O (2007) Markers and methods for cell sorting of human embryonic stem cell-derived neural cell populations. *Stem Cells* 25:2257–2268.
36. Brustle O, Maskos U, McKay RD (1995) Host-guided migration allows targeted introduction of neurons into the embryonic brain. *Neuron* 15:1275–1285.
37. Gaiano N, Fishell G (1998) Transplantation as a tool to study progenitors within the vertebrate nervous system. *J Neurobiol* 36:152–161.
38. Wernig M, *et al*. (2004) Functional integration of embryonic stem cell-derived neurons *in vivo*. *J Neurosci* 24:5258–5268.
39. Bjorklund LM, *et al*. (2002) Embryonic stem cells develop into functional dopaminergic neurons after transplantation in a Parkinson rat model. *Proc Natl Acad Sci USA* 99:2344–2349.
40. Brustle O, *et al*. (1997) *In vitro*-generated neural precursors participate in mammalian brain development. *Proc Natl Acad Sci USA* 94:14809–14814.
41. Muotri AR, Nakashima K, Toni N, Sandler VM, Gage FH (2005) Development of functional human embryonic stem cell-derived neurons in mouse brain. *Proc Natl Acad Sci USA* 102:18644–18648.